Hyperbolic Conservation Laws with Source Terms: Errors of the Shock Location

P. Klingenstein

Research Report No. 94-07
August 1994

Seminar für Angewandte Mathematik
Eidgenössische Technische Hochschule
CH-8092 Zürich
Switzerland

Hyperbolic Conservation Laws with Source Terms: Errors of the Shock Location[1]

P. Klingenstein

Seminar für Angewandte Mathematik
Eidgenössische Technische Hochschule
CH-8092 Zürich
Switzerland

Research Report No. 94-07 August 1994

Abstract

We investigate the error of the shock location which occurs in numerical solutions of hyperbolic conservation laws with source terms. For our theoretical analysis we consider a scalar Riemann problem. We compute its solution using a splitting method. This means that in each time step the homogeneous conservation law and an ODE (modeling the source term) are solved separately. We show that the local error of the shock location can be considered to consist of two parts: one part introduced by the splitting and another occurring because of smeared-out shock profiles.

Numerical examples show that these error-estimates can be used to adapt the step size so that the error of the shock location remains sufficiently small. The numerical examples include one-dimensional systems.

[1]Talk at the Fifth International Conference on Hyperbolic Problems, June, 13-17, 1994, University at Stony Brook, New York.

1 Introduction

When computing numerical solutions of hyperbolic conservation laws with source terms, one may obtain spurious solutions — solutions which seem to be correct but which are totally unphysical such as shock waves moving with wrong speeds [3][1]. Therefore it is important to know how errors of the shock location can be estimated. This is the aim of our investigation in the first part of this paper. We are interested in the errors of the shock location of numerical solutions which are computed using a splitting method. This means that in each time step the homogeneous conservation law and an ODE (modeling the source term) are solved separately. We consider a scalar Riemann problem in Section 2 to get error-estimates. First we analyze the local error considering solutions with sharp shock profiles and then we look at solutions with smeared-out shock profiles. In Section 3 these error-estimates are used to construct an adaptation of the step size so that the error of the shock location remains sufficiently small. The numerical examples which include a scalar problem (Burgers' equation with a linear source term) and the simplified combustion model introduced by A. Majda [1] show that the adaptation based on the error-estimates for the scalar Riemann problem derived in Section 2 gives satisfactory results.

2 Theoretical analysis

In this section we investigate the local error of the shock location considering a one-dimensional scalar Riemann problem:

$$u_t + f(u)_x = q(u)$$

$$u(x,0) = \begin{cases} u_l, & x < x_0 \\ u_r, & x > x_0 \end{cases} .$$

f and q are assumed to be smooth functions of u where $u(x,t) : I\!R \times I\!R_+ \to I\!R$ and $q^{(n)} =: \mu\tilde{q}^{(n)}$ with $\tilde{q}^{(n)} = O(1)$, $n = 0, 1, \ldots$. This restriction on q is not necessary to get the error-estimates — it just determines the higher order terms. The conditions for the existence of a shock (at least in the time interval $[t_n, t_{n+1}]$) should be fulfilled.

Solution operators:

The solution operator for the homogeneous conservation law $u_t + f(u)_x = 0$ is called 'L_f' and the one for the ODE $u_t = q(u)$ 'L_q'. The numerical solution is computed using the **Strang splitting** which is defined as follows:

$$u^{n+1} = (\tfrac{1}{2}L_q \; L_f \; \tfrac{1}{2}L_q)u^n. \tag{1}$$

Here $\frac{1}{2}L_q$ signifies that L_q is applied for half a time step and u^n is the numerical solution at time t_n. In a Riemann problem a step function $u(x,t)$ is given. The values of $u(x,t)$ on the left resp. right side of the discontinuity only depend on t. We denote them by $u_l(t)$ resp. $u_r(t)$.

- If we apply L_q then L_q only changes the quantities u_l and u_r. Of course, in solutions with smeared-out shock profiles, L_q would influence the intermediate values, too.

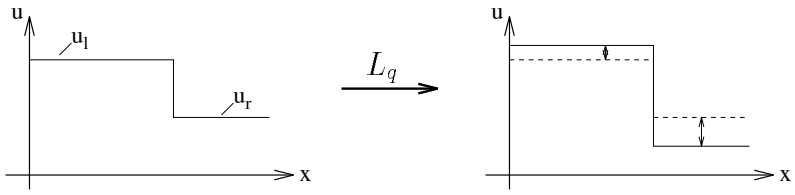

- If we apply L_f then just the discontinuity is propagated. If L_f produces smeared-out shock profiles, we can determine the shock location using the 'equal area rule' due to conservation.

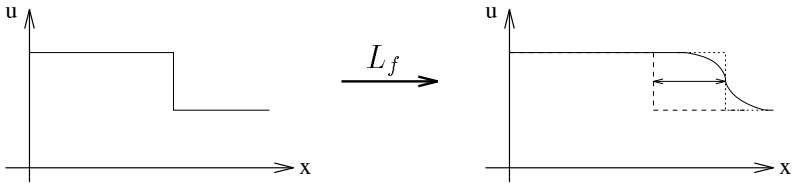

2.1 Solutions with sharp shock profiles

Now L_f and L_q are considered to be the *exact solution operators*. Then the shock profiles are not smeared out and the quantities $u_l(t)$ and $u_r(t)$ are exact. In this case the local error of the shock location can be considered to be the *local splitting error* because the solution operators are exact.

To investigate this local splitting error, we assume the shock location σ^n of the numerical solution at time t_n to be correct. We use the Rankine Hugoniot jump condition

$$\dot{\sigma}(t) = \frac{f(u_l(t)) - f(u_r(t))}{u_l(t) - u_r(t)} =: h(u_l, u_r) \tag{2}$$

where $\sigma(t)$ is the shock location of the exact solution. The function h is the shock speed and we denote h^n to be $h^n := h(u_l^n, u_r^n)$.

Defining $\triangle\sigma$ as the difference $\triangle\sigma := \sigma^{n+1} - \sigma^n$ and noticing that

$$\triangle\sigma_{num} - \triangle\sigma_{exact} = [\sigma_{num}^{n+1} - \sigma_{num}^n] - [\sigma_{exact}^{n+1} - \sigma_{exact}^n] = \sigma_{num}^{n+1} - \sigma_{exact}^{n+1}$$

we write the local error as $\triangle\sigma_{num} - \triangle\sigma_{exact}$. By means of the Taylor series expansion we find that *local splitting error* is

$$\begin{aligned} \mathcal{E}_{spl} &:= \triangle\sigma_{num} - \triangle\sigma_{exact} \\ &= (\tfrac{1}{2} - \theta)\triangle t^2 \left[h_{u_l}^n \, q(u_l^n) + h_{u_r}^n \, q(u_r^n) \right] + (\tfrac{1}{2} - \theta) \cdot O(\mu^2 \triangle t^3) \\ &\quad \text{where } \theta \in (0,1). \end{aligned} \tag{3}$$

Remarks:

- If L_q is not the exact solution operator but one with a local truncation error of the order p: $u^{n+1} - u(t_{n+1}) = O((\mu\triangle t)^p)$ then an additional error $O(\mu^p \triangle t^{p+1})$ occurs in $\mathcal{E}_{spl}$.
- If L_f is any consistent solution operator in conservation form then no additional error occurs.

2.2 Solutions with smeared-out shock profiles

To complete the analysis we now consider numerical solutions with smeared-out shock profiles. Therefore we assume L_f to be a conservative solution operator which produces smearing. L_q and σ^n are exact.

Let us look at one time step of the Strang splitting procedure:

- We start with the function u^n with a smeared-out shock profile:

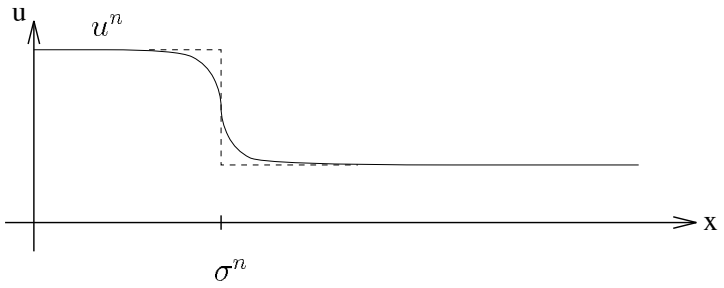

The shock location is determined by the equal area rule.

- Then a half time step L_q is applied. We get $u^{n+\frac{1}{2}}$:

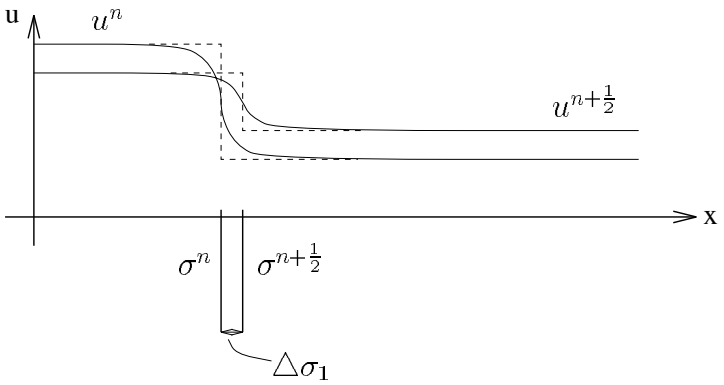

L_q works on the values on the left and on the right sides of the shock *but it also works on the intermediate values.* This causes a change in the shock profile and therefore, in general, a change in the shock location: $\triangle\sigma_1$.

- Now one time step L_f is applied and we get $\bar{u}^{n+\frac{1}{2}}$:

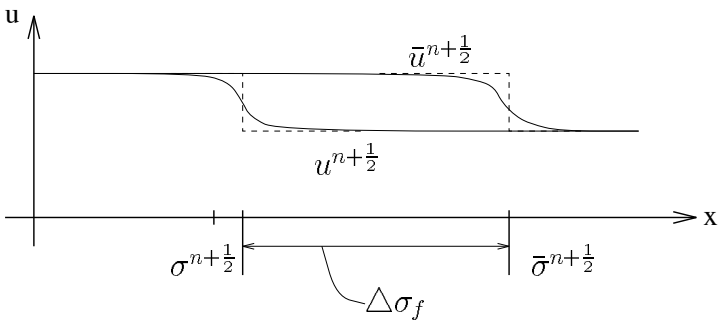

  L_f changes the shock location due to conservation — according to the (exact) values $u_l^{n+\frac{1}{2}}$, $u_r^{n+\frac{1}{2}}$: The change in the shock location is denoted by $\triangle\sigma_f$.

- Again a half time step L_q is applied. We get u^{n+1}:

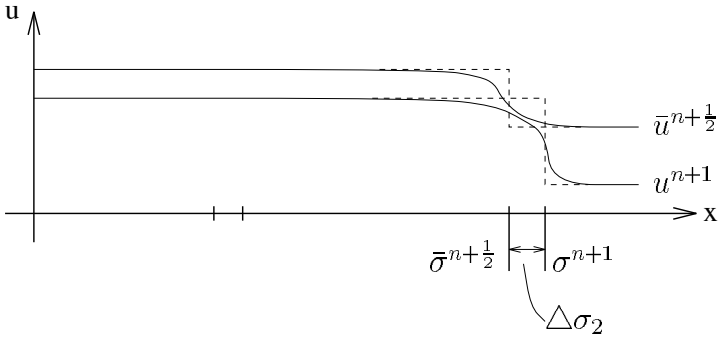

  The change in the shock location is denoted by $\triangle\sigma_2$.

The numerical shock location changes over one time step by

$$\triangle\sigma_{num} = \triangle\sigma_1 + \triangle\sigma_f + \triangle\sigma_2$$

and the formula for the local error of the shock location calculates as

$$\boxed{\mathcal{E} := \triangle\sigma_{num} - \triangle\sigma_{exact} = \triangle\sigma_1 + \triangle\sigma_2 + \underbrace{\triangle\sigma_f - \triangle\sigma_{exact}}_{\mathcal{E}_{spl}}} \tag{4}$$

where the difference of the last two terms is already known: It is the error that occurs in the solution with sharp discontinuities. So only the quantities $\triangle\sigma_1$ and $\triangle\sigma_2$ are left to be determined.

Influence of smearing:

Considering the numerical solution at time t_n we assume the shock location to be correct and determine it by the equal area rule:

$$\int_{\sigma^n-\epsilon}^{\sigma^n+\epsilon} u^n dx = \epsilon(u_l^n + u_r^n).$$

Here ϵ is assumed to be the width of the smearing of the shock profile.

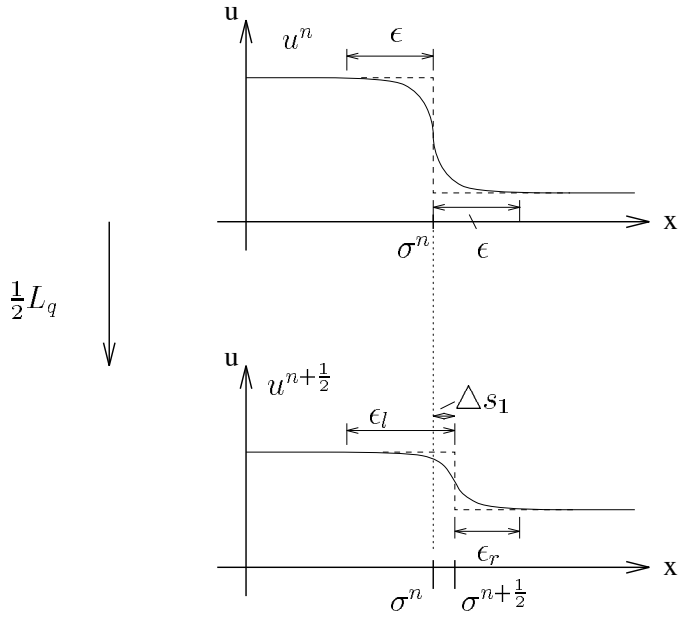

After applying $\frac{1}{2}L_q$ we get

$$\int_{\sigma^n-\epsilon}^{\sigma^n+\epsilon} u^{n+\frac{1}{2}}dx = \epsilon_l u_l^{n+\frac{1}{2}} + \epsilon_r u_r^{n+\frac{1}{2}} = (\epsilon + \triangle\sigma_1)u_l^{n+\frac{1}{2}} + (\epsilon - \triangle\sigma_1)u_r^{n+\frac{1}{2}}.$$

By definition of ϵ we have $\triangle\sigma_1 < \epsilon$. Taking into account that

$$u^{n+\frac{1}{2}} - u^n = \frac{\triangle t}{2}q(u^n) + \frac{\triangle t^2}{8}q'(u^n)q(u^n) + O(\mu^3\triangle t^3)$$

and defining

$$\delta(u) := \frac{\triangle t}{2}q(u) + \frac{\triangle t^2}{8}q'(u)q(u),$$

we get

$$\int_{\sigma^n-\epsilon}^{\sigma^n+\epsilon}(u^{n+\frac{1}{2}} - u^n)dx = \int_{\sigma^n-\epsilon}^{\sigma^n+\epsilon}\delta(u^n)dx + O(\epsilon\mu^3\triangle t^3) = 2\epsilon\delta(u_*^n) + O(\epsilon\mu^3\triangle t^3) \qquad (5)$$

where $u_*^n \in (\max_x u^n(x), \min_x u^n(x))$. Rearranging terms and summing up all the higher order terms in the expression $O(\ldots)$, we get the following result:

$$\boxed{\triangle\sigma_1 = \epsilon\frac{2\delta(u_*^n) - \delta(u_l^n) - \delta(u_r^n)}{u_l^n - u_r^n + \delta(u_l^n) - \delta(u_r^n)} + O(\epsilon\mu^3\triangle t^3).} \qquad (6)$$

If we replace u^n by $\bar{u}^{n+\frac{1}{2}}$, we get $\triangle\sigma_2$. So the error analysis is complete.

3 Numerical applications

In this section we test by means of numerical examples how far the error-estimates derived in the previous section can be used to adapt the step size so that the error of the shock location remains sufficiently small. We show two examples — a scalar problem and a simplified combustion model.

3.1 The scalar example

We consider Burgers' equation with a linear source term:

$$u_t + (\frac{1}{2}u^2)_x = -\mu(u-a)$$

where

$$a := \begin{cases} 1, & u \geq 0.25 \\ 0, & u < 0.25 \end{cases} .$$

The initial data define a Riemann problem

$$u(x,0) = \begin{cases} 1, & x < 0 \\ 0, & x > 0 \end{cases} .$$

The source term shifts values of u which are greater than 0.25 towards 1 and values which are less than 0.25 towards 0. With the given initial data the source is equal to zero on both sides of the shock. The exact solution is

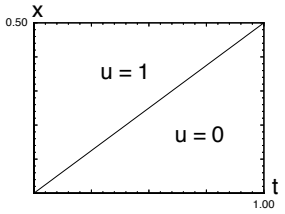

$$u(x,t) = u(x - \tfrac{1}{2}t, 0) .$$

3.1.1 Numerical wave speeds

The numerical solution is computed using the Strang splitting. The homogeneous conservation law is solved with an upwind scheme and the ODE is solved with the implicit Euler scheme. Because the solution does not depend on $\triangle t$ but on $\mu\triangle t$, the step sizes are fixed and only the relative time $T_{rel} := \mu\triangle t$ is varied. We get the following results (see Fig. 1):

- For T_{rel} small the shock speed is correct.
- If we increase T_{rel}, the shock speed becomes wrong.
- If T_{rel} is large enough, two phenomena occur:
  - For ratios of the step sizes $\frac{\triangle t}{\triangle x} < 0.5$ the discontinuity does not move at all.
  - For $\frac{\triangle t}{\triangle x} > 0.5$ the discontinuity moves one grid cell per time step.

These phenomena occur because of the smearing of the shock profile. Let us look at the single steps of the Strang splitting procedure (see Fig. 2):

- In the first step nothing happens: $q(u_i^n) = 0 \quad \forall i.$

Figure 1: Shock curves of the numerical solutions for different T_{rel}, $\frac{\triangle t}{\triangle x} = 0.45$ or $\frac{\triangle t}{\triangle x} = 0.55$, and $\triangle t = 0.01$.

$\frac{\triangle t}{\triangle x} = 0.45$:

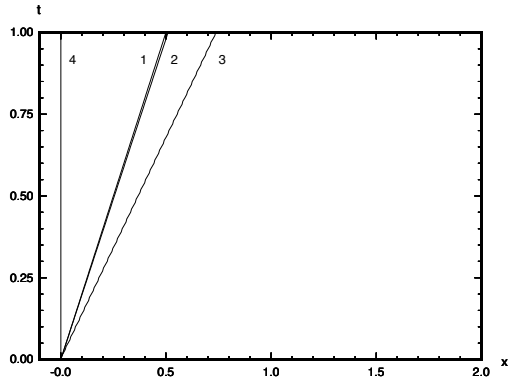

$\frac{\triangle t}{\triangle x} = 0.55$:

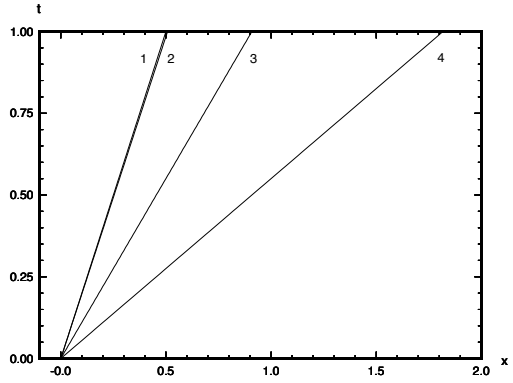

$1:\ T_{rel} = 0.00001\,, \quad 2:\ T_{rel} = 0.01\,, \quad 3:\ T_{rel} = 1\,, \quad 4:\ T_{rel} = 100.$

- In the second step the upwind scheme produces one intermediate value. For ratios $\frac{\triangle t}{\triangle x} < 0.5$ this value is less than 0.25 and for $\frac{\triangle t}{\triangle x} > 0.5$ it is greater than 0.25.
  We consider the first case.

- For $\frac{\triangle t}{\triangle x} < 0.5$ the intermediate value is less than 0.25 so L_q shifts this value towards zero.

- In the next time step $\frac{1}{2}L_q$ is applied first. The intermediate value is shifted again towards zero.

If T_{rel} is large enough, the intermediate value is shifted so close to zero that after one time step the discontinuity has not moved at all. The case $\frac{\triangle t}{\triangle x} > 0.5$ behaves analogously.

Figure 2: The three steps of the Strang splitting (over one time step) for $T_{rel} = 100$ and $\frac{\triangle t}{\triangle x} = 0.45$.

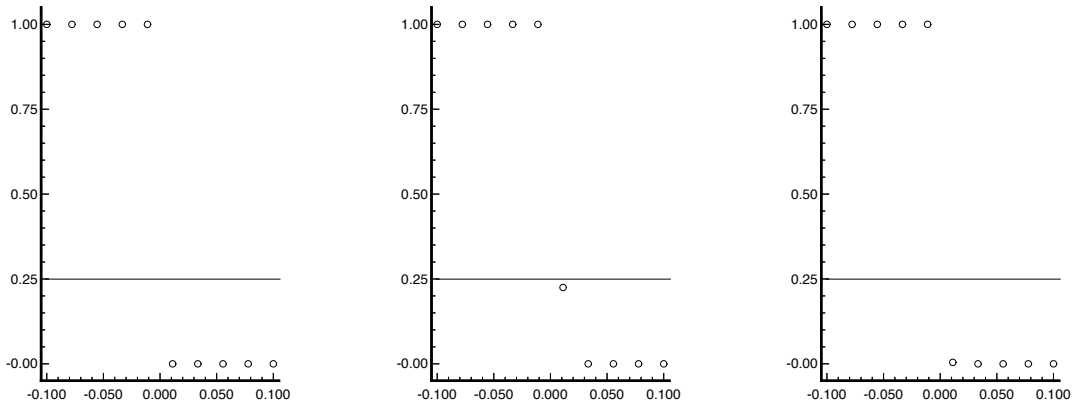

3.1.2 Local errors

First we have to decide how the changes of the shock location over one time step are to be computed in this example. For the exact solution we have

$$\triangle\sigma_{exact} = \frac{1}{2}\triangle t$$

and for the numerical solution we can write

$$\triangle\sigma_{num} = \triangle x \sum_i (u_i^{n+1} - u_i^n)$$

where u_i^n is the numerical solution at time t_n and location x_i. The local error of the shock location is the difference of these two expressions

$$\boxed{\mathcal{E} := \triangle\sigma_{num} - \triangle\sigma_{exact} = \triangle x \sum_i (u_i^{n+1} - u_i^n) - \frac{1}{2}\triangle t.} \tag{7}$$

Now we want to test if the error-estimates derived in Section 2 are sufficiently exact when the remaining terms of higher order are neglected. The local error can be written as in (4). It reduces in the considered problem to

$$\mathcal{E} = \triangle\sigma_1 + \triangle\sigma_2$$

because with the special choice of the source term $\mathcal{E}_{spl} = 0$. Also $\triangle\sigma_1$ reduces to

$$\triangle\sigma_1 = 2\epsilon\delta(u_*^n) + O(\epsilon\mu^3\triangle t^3)$$

as $\delta(u_l^n) = \delta(u_r^n) = 0$ and $u_l^n - u_r^n = 1$. The same holds for $\triangle\sigma_2$ (replacing u^n by $\bar{u}^{n+\frac{1}{2}}$).

To compute $\triangle\sigma_1$ and $\triangle\sigma_2$ we remember (5)

$$2\epsilon\delta(u_*^n) = \int_{\sigma^n-\epsilon}^{\sigma^n+\epsilon} \delta(u^n)dx.$$

Because of

$$\delta(u) = (u-a)\left[\frac{1}{8}(\mu\triangle t)^2 - \frac{1}{2}\mu\triangle t\right]$$

(a depending on u) we have

$$\int_{\sigma^n-\epsilon}^{\sigma^n+\epsilon} \delta(u^n)dx = \int_{x_-}^{x_+} \delta(u^n)dx \quad , \text{ for any } x_- \le \sigma^n - \epsilon \text{ and } x_+ \ge \sigma^n + \epsilon.$$

Defining u_i^n to be the cell average

$$u_i^n = \frac{1}{\triangle x}\int_{x_{i-\frac{1}{2}}}^{x_{i+\frac{1}{2}}} u(x,t_n)dx,$$

we get

$$\triangle\sigma_1 + \triangle\sigma_2 = \triangle x \sum_i \left[\delta(u_i^n) + \delta(\bar{u}_i^{n+\frac{1}{2}})\right] + O(\epsilon\mu^3\triangle t^3). \tag{8}$$

Dropping the higher order terms, we calculate the estimated error as

$$\boxed{\mathcal{E}_{est} := \triangle x \sum_i \left[\delta\left(u_i^n\right) + \delta\left(\bar{u}_i^{n+\frac{1}{2}}\right)\right].} \tag{9}$$

In our numerical computations the relative time T_{rel} is varied. The step sizes $\triangle t$ and $\triangle x$ are fixed and we look at the solutions at time $T = t_N = 1$. The relative (global) error

$$E_{rel} := \frac{|\sigma^N - \sigma(t_N)|}{|\sigma(t_N)|},$$

the maximum of the local errors, and the maximum of the differences between the estimated and the exact local error are shown in the table below:

T_{rel}	E_{rel}	max($\mathcal{E}$)	max($\mathcal{E}_{est}$)	Difference
0.1 E-02	0.159448E-02	0.146037E-04	0.146037E-04	0.608730E-12
0.2 E-02	0.317808E-02	0.288762E-04	0.288762E-04	0.481385E-11
0.3 E-02	0.476176E-02	0.435261E-04	0.435261E-04	0.163281E-10
0.4 E-02	0.633019E-02	0.577346E-04	0.577346E-04	0.385089E-10
0.5 E-02	0.806836E-02	0.731136E-04	0.731135E-04	0.762074E-10
0.6 E-02	0.929683E-02	0.842295E-04	0.842294E-04	0.126439E-09
0.7 E-02	0.110235E-01	0.101773E-03	0.101773E-03	0.207968E-09
0.8 E-02	0.125525E-01	0.116287E-03	0.116287E-03	0.310409E-09
0.9 E-02	0.138511E-01	0.128711E-03	0.128710E-03	0.434888E-09
1.0 E-02	0.157083E-01	0.144855E-03	0.144854E-03	0.604318E-09

The errors depend linearly on T_{rel} — this is obvious as the spatial step size is not refined. All the differences between the estimated and the exact local error are so small that we conclude that the estimation formula is sufficiently exact.

3.1.3 Adaptation

Now we are ready to test if an adaptation based on $\mathcal{E}_{est}$ gives satisfactory results. This adaptation works as follows: The estimated local error of the shock location $\mathcal{E}_{est}$ is expected to be smaller than a certain upper bound B. If this assumption is not satisfied, the step sizes $\triangle t$ and $\triangle x$ are bisected so that the ratio $\frac{\triangle t}{\triangle x}$ stays constant.

We define the upper bound for the local error to be

$$B := 0.5 \cdot \triangle t \cdot c_0 \cdot 0.01\,, \qquad c_0 := \begin{cases} 1, & b_0 \leq 3 \\ b_0, & 4 \leq b_0 \leq 8 \\ b_0 + 1, & 9 \leq b_0 \end{cases}$$

where b_0 is the number of bisections. Notice that the factor 0.5 is the shock speed. We choose $\epsilon = 0.1$. As before we look at solutions at time $T = 1$. In the table below you see the various step sizes $\triangle t^0$ at time $t = 0$, the number of bisections and time steps, the resulting smallest $\triangle t$, and the relative error of the shock location.

$\triangle t^0$	#(bisections)	#(time steps)	Resulting $\triangle t$	E_{rel}
0.01	4	1601	0.625000E-03	0.100392E-01
0.10	8	2554	0.396250E-03	0.676327E-02
0.20	8	1278	0.761250E-03	0.129742E-01
1.00	11	2020	0.488281E-03	0.945125E-02
2.00	12	1901	0.488281E-03	0.128107E-01

The resulting step sizes are all about the same size and the relative error remains less than 1.3%.

3.2 The combustion model

We consider a simplified model for the inviscid reacting compressible Euler equations in one space dimension. This model is a (2×2) - system, given by Burgers' equation coupled to a chemical kinetics equation. It has analogues in the Z-N-D theory and the structure of the reacting shock profiles (see [1] or [4] for more details). Therefore we use it as a first test example to investigate if an adaptation based on the estimation formula (4) would also work for combustion problems.

The model equations are given by

$$\begin{aligned} u_t + (\tfrac{1}{2}u^2 - q_0 Z)_x &= 0 \\ Z_x &= \Phi(u) Z \end{aligned}$$

with initial data

$$u(x,0) = \begin{cases} 1.0, & x > 0 \\ -0.7, & x < 0 \end{cases} .$$

We use ignition temperature kinetics so that the function $\Phi(u)$ is given as

$$\Phi(u) = \begin{cases} 1, & u \geq 0 \\ 0, & u < 0 \end{cases} .$$

Z is the mass fraction of unburned gas with $\lim_{x\to\infty} Z(x,t) = 1$. We set $q_0 = 0.935$ where q_0 is the heat release.

The initial data are chosen such that the speed of the combustion wave at time $t = 0$ is $\dot{\sigma}(0) = 0.15$ and a traveling wave solution evolves with a fixed speed $\dot{\sigma}(t) = 0.7$. The solution u exhibits a combustion spike. In Figure 3 the solution profiles of u and Z at time $T = 10$ and also the shock curve are shown.

Figure 3: Reference solution of the simplified combustion model showing u, Z at time $T = 10$ and the shock curve.

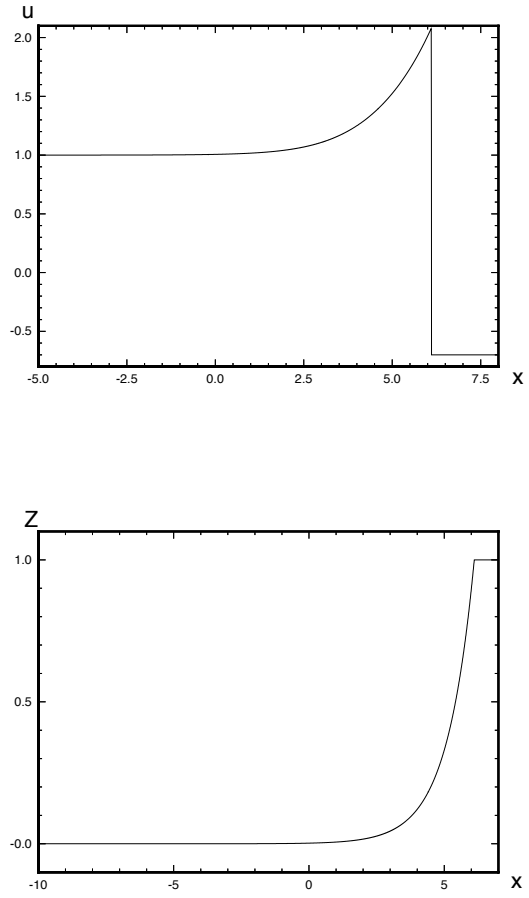

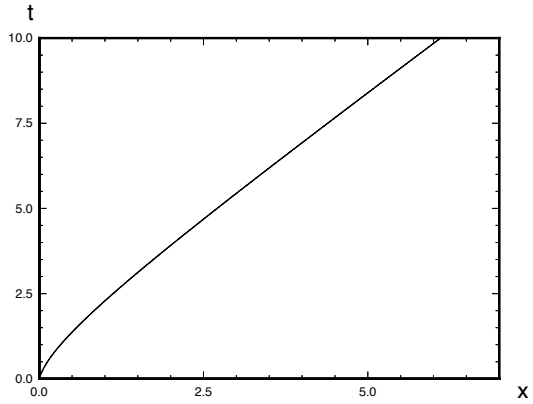

3.2.1 Numerical wave speeds

The numerical solution is computed using the Strang splitting where the equations

$$u_t + (\frac{1}{2}u^2)_x = 0 \tag{10}$$

$$Z_x = \Phi(u)Z \tag{11}$$

$$u_t = q_0\Phi(u)Z \tag{12}$$

are solved separately in each time step. Equation (10) is solved with an upwind scheme as in the case of the scalar example, equation (11) is solved by trapezoidal approximation of the integral in the exact solution formula, and equation (12) is solved exactly. For different step sizes $\triangle t$ (with $\frac{\triangle t}{\triangle x} = const.$) the solution shows the following behaviour for the combustion wave speeds (see Fig. 4):

- For $\triangle t$ small the shock speed is correct.
- If we increase $\triangle t$, the shock speed becomes slower than the correct speed.
- If $\triangle t$ is large enough, the shock speed remains unchanged: $\dot{\sigma}(t) \equiv \dot{\sigma}(0) = 0.15$.

This phenomenon occurs because the combustion spike of the solution decreases when the step size is increased.

Figure 4: Numerical solution of the simplified combustion model showing u after 1000 time steps and the shock curve for different $\triangle t$.

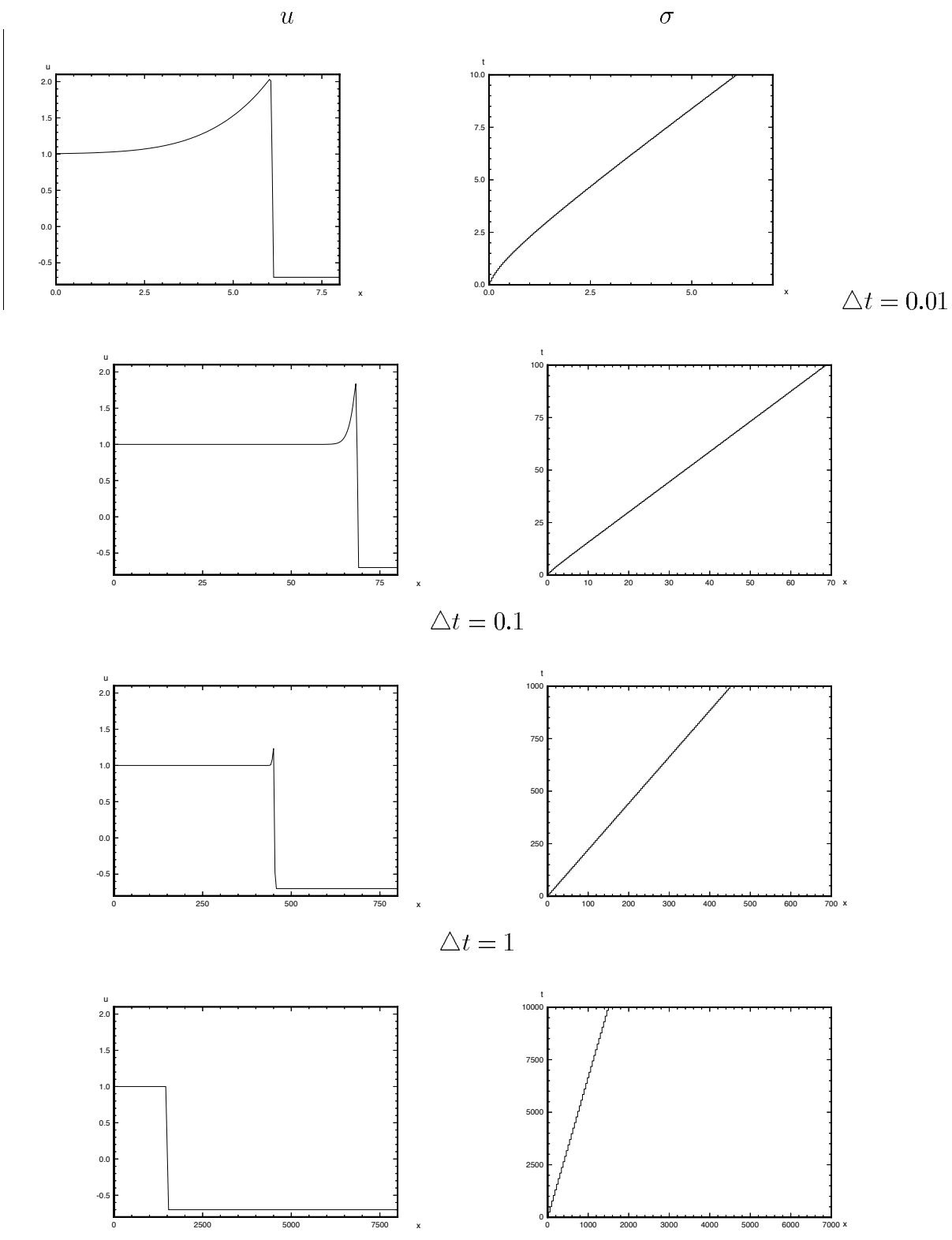

3.2.2 Local errors

Again we have to decide how the local error of the shock location (given by (4))

$$\mathcal{E} := \triangle\sigma_{num} - \triangle\sigma_{exact} = \triangle\sigma_1 + \triangle\sigma_2 + \underbrace{\triangle\sigma_f - \triangle\sigma_{exact}}_{\mathcal{E}_{spl}}$$

is to be approximated. Let us first consider $\mathcal{E}_{spl}$. In (3) we drop the higher order terms. Equation (10) defines

$$h(u_l, u_r) = \frac{1}{2}(u_l + u_r) \quad \text{with} \quad h_{u_l} = h_{u_r} = \frac{1}{2}.$$

Equation (12) gives

$$q(u) = q_0 \Phi(u) Z \quad \text{with} \quad q(u_r) = 0\,, \quad q(u_l) = q_0$$

where, for the sake of simplicity, Z is assumed to not depend locally on t. Dropping higher order terms in (3) we set the following inequality for $\tilde{\mathcal{E}}_{spl}$:

$$\begin{aligned} |\tilde{\mathcal{E}}_{spl}| &:= |\mathcal{E}_{spl} + (\tfrac{1}{2} - \theta) \cdot O(\mu^2 \triangle t^3)| \\ &= |(\tfrac{1}{2} - \theta)\triangle t^2 \cdot \tfrac{1}{2} \cdot q_0| \\ &< \tfrac{1}{4} q_0 \triangle t^2\,. \end{aligned} \tag{13}$$

To approximate $\triangle\sigma_1$ and $\triangle\sigma_2$ we define the region of the smearing (x_L, x_R) as

$$x_L := x_{k_L}\,, \quad x_R := x_{k_R}$$

where k_L, k_R are defined such that

$$k_L \,:\, u_{k_L} = \max_i u_i \quad \text{and} \quad k_R := \min\{i \,|\, u_i = u_r\,\}.$$

Using $q' = 0$ we get

$$\delta(u) = \frac{1}{2}\triangle t\, \Phi(u)\, q_0 Z. \tag{14}$$

For $x \geq \sigma(t)$ we have $Z \equiv 1$ and we approximate Z by $Z \equiv 1$ over the region of the smearing (x_L, x_R). Then (14) gives

$$\delta(u) = \begin{cases} \frac{1}{2} q_0 \triangle t, & u \geq 0 \\ 0, & u < 0 \end{cases}, \; x \in (x_L, x_R). \tag{15}$$

We use the equal area rule to compute the shock location $\sigma := x_{k_\sigma}$ (where the values of u on the left and right sides of the shock are u_{k_L} and u_{k_R} and $k_\sigma \in I\!R$). We define k_0 to be the largest index for which $u_i \geq 0$.

Now we are ready to compute $\triangle\sigma_1$ and $\triangle\sigma_2$ as

$$\triangle\sigma_1 = \frac{\frac{1}{2}(k_0^n - k_\sigma^n)q_0\triangle x\triangle t}{u_{k_L}^n - u_{k_R}^n + \frac{1}{2}q_0\triangle t}, \quad \triangle\sigma_2 = \frac{\frac{1}{2}(\bar{k}_0^{n+\frac{1}{2}} - \bar{k}_\sigma^{n+\frac{1}{2}})q_0\triangle x\triangle t}{\bar{u}_{k_L}^{n+\frac{1}{2}} - \bar{u}_{k_R}^{n+\frac{1}{2}} + \frac{1}{2}q_0\triangle t}.$$

Summing up the above results we estimate the local error of the shock location by

$$\boxed{\mathcal{E}_{est} := |\triangle s_1 + \triangle s_2| + \frac{1}{4}q_0\triangle t^2.} \tag{16}$$

3.2.3 Adaptation

Now we test if an adaptation based on $\mathcal{E}_{est}$ gives satisfactory results. If $\mathcal{E}_{est}$ is not smaller than a certain upper bound B, the step sizes $\triangle t$ and $\triangle x$ are bisected so that the ratio $\frac{\triangle t}{\triangle x}$ stays constant.

We set the upper bound for the local error to be

$$B := 0.01 \cdot \triangle t.$$

We look at solutions at time $T = t_N = 10$. Listed in the table below are the various step sizes $\triangle t^0$ at time $t = 0$, the number of bisections and time steps, the resulting smallest $\triangle t$, and the relative (global) error of the shock location which is now defined by

$$E_{rel} := \frac{|\sum_{n=0}^{N-1}(\triangle\sigma_{num} - \triangle\sigma_{exact})^n|}{|\sigma^N|}.$$

.

$\triangle t^0$	#(bisections)	#(time steps)	Resulting $\triangle t$	E_{rel}
0.1	5	3199	0.312500E-02	0.550740E-02
1.0	8	2560	0.390625E-02	0.694970E-02
2.0	9	2560	0.390625E-02	0.694970E-02
5.0	11	4090	0.244141E-02	0.432801E-02
10.	12	4090	0.244141E-02	0.432801E-02
20.	13	4090	0.244141E-02	0.432801E-02

The resulting step sizes are all about the same size and the relative errors remain less than 0.7%.

4 Conclusions

We have analyzed the local error of the shock location for a scalar one-dimensional Riemann problem and computed two numerical examples. We have estimated the local errors of the shock location in the numerical computations and shown that an adaptation of the step size based on these estimates works well.

Using our experiences with the simplified combustion model we are next going to test an adaptation for the inviscid reacting compressible Euler equations in one space dimension.

References

[1] P. Colella, A. Majda, and V. Roytburd. Theoretical and numerical structure for reacting shock waves. *SIAM J. Sci. Stat. Comput.*, 4:1059–1080, 1986.

[2] R. J. LeVeque. *Numerical Methods for Conservation Laws*. Lectures in Mathematics, ETH Zürich, Birkhäuser, 1992.

[3] R. J. LeVeque and H. C. Yee. A study of numerical methods for hyperbolic conservation laws with stiff source terms. *J. Comput. Phys.*, 86:187 – 210, 1990.

[4] A. Majda. A qualitative model for dynamic combustion. *SIAM J. Appl. Math.*, 41:50 – 93, 1981.

[5] G. Strang. On the construction and comparison of difference schemes. *SIAM J. Numer. Anal.*, 5:506–517, 1968.

[6] H. C. Yee. *A class of high-resolution explicit and implicit shock-capturing methods*. NASA Technical Memorandum 101088, 1989.

Research Reports

No.	Authors	Title
94-07	P. Klingenstein	Hyperbolic conservation laws with source terms: Errors of the shock location
94-06	M.D. Buhmann	Multiquadric Pre-Wavelets on Non-Equally Spaced Centres
94-05	K. Burrage, A. Williams, J. Erhel, B. Pohl	The implementation of a Generalized Cross Validation algorithm using deflation techniques for linear systems
94-04	J. Erhel, K. Burrage, B. Pohl	Restarted GMRES preconditioned by deflation
94-03	L. Lau, M. Rezny, J. Belward, K. Burrage, B. Pohl	ADVISE - Agricultural Developmental Visualisation Interactive Software Environment
94-02	K. Burrage, J. Erhel, B. Pohl	A deflation technique for linear systems of equations
94-01	R. Sperb	An alternative to Ewald sums
93-07	R. Sperb	Isoperimetric Inequalities in a Boundary Value Problem in an Unbounded Domain
93-06	R. Sperb	Extension and simple Proof of Lekner's Summation Formula for Coulomb Forces
93-05	A. Frommer, B. Pohl	A Comparison Result for Multisplittings Based on Overlapping Blocks and its Application to Waveform Relaxation Methods
93-04	M. Pirovino	The Inverse Sturm-Liouville Problem and Finite Differences
93-03	R. Jeltsch, X. Wang	Uniqueness of Piecewise Lipschitz Continuous Solutions of the Cauchy-Problem for 2×2 Conservation Laws
93-02	W.-A. Yong	Difference approximations to the global $W^{1,\infty}$ solutions of the isentropic gas equations
93-01	Ch. Lubich, K. Nipp, D. Stoffer	Runge-Kutta solutions of stiff differential equations near stationary points
92-15	N. Botta	Is the transonic flow around a cylinder always periodic?
92-14	K. Nipp, D. Stoffer	Invariant manifolds of numerical integration schemes applied to stiff systems of singular perturbation type - Part I: RK-methods
92-13	K. Nipp	Smooth attractive invariant manifolds of singularly perturbed ODE's
92-12	D. Mao	A Shock Tracking Technique Based on Conservation in One Space Dimension